HOKKAIDO UNIVERSITY

Title	Experimental determination of the excitation functions of the alpha particle-induced nuclear reactions on rhodium up to 50 MeV
Author(s)	Ditrói, Ferenc; Takács, Sándor; Haba, Hiromitsu et al.
Citation	European physical journal. A, Hadrons and nuclei, 61(9), 201 https://doi.org/10.1140/epja/s10050-025-01670-x
Issue Date	2025-09
Doc URL	https://hdl.handle.net/2115/98059
Rights	© The Author(s) 2025
Rights(URL)	https://creativecommons.org/licenses/by/4.0/
Type	journal article
File Information	Euro_Phys_J_A_61_2025.pdf

Hokkaido University Collection of Scholarly and Academic Papers : HUSCAP

Eur. Phys. J. A (2025) 61:201
https://doi.org/10.1140/epja/s10050-025-01670-x

THE EUROPEAN PHYSICAL JOURNAL A

Regular Article - Experimental Physics

Experimental determination of the excitation functions of the alpha particle-induced nuclear reactions on rhodium up to 50 MeV

Ferenc Ditrói[1,a], Sándor Takács[1], Hiromitsu Haba[2], Masayuki Aikawa[3,4,5], He Huang[4], Zolbadral Tsoodol[7], Kenta Sugihara[8,9], Shuichiro Ebata[6], Zoltán Szűcs[1], Tamás Tornyi[1]

[1] HUN-REN Institute for Nuclear Research (ATOMKI), 4026 Debrecen, Hungary
[2] Nishina Center for Accelerator-Based Science, RIKEN, Wako 351-0198, Japan
[3] Faculty of Science, Hokkaido University, Sapporo 060-0810, Japan
[4] Graduate School of Biomedical Science and Engineering, Hokkaido University, Sapporo 060-8638, Japan
[5] Global Center for Biomedical Science and Engineering, Faculty of Medicine, Hokkaido University, Sapporo 060-8648, Japan
[6] Graduate School of Science and Engineering, Saitama University, Saitama 338-8570, Japan
[7] Nuclear Research Center, National University of Mongolia, Ulaanbaatar 13330, Mongolia
[8] High Energy Accelerator Research Organization (KEK), Oho, Tsukuba, Ibaraki 305-0801, Japan
[9] The Graduate University for Advanced Studies (SOKENDAI), Hayama, Kanagawa 240-0193, Japan

Received: 19 June 2025 / Accepted: 20 August 2025
© The Author(s) 2025
Communicated by Aurora Tumino.

Abstract Natural rhodium foils were irradiated with 50 MeV alpha particles to determine the excitation functions for forming medically and industrially relevant radioisotopes of silver and rhodium using the stacked foil activation technique. Cross sections for producing ^{103,104g,105,106m}Ag and ^{100,101m,102m,g}Rh were determined from the thresholds to the maximum bombarding energy. The results were compared with the cross section calculations from the TENDL-2023 online database.

1 Introduction

This study aims to measure the cross sections of alpha particle-induced nuclear reactions on natural rhodium metal targets to resolve disagreements between previous data and determine new cross sections. Rhodium (monoisotopic ^{103}Rh) is a transition metal that is generally chemically inert, and it does not react easily with other substances. This makes it relatively safe to handle in solid form. In industrial settings, where rhodium is used as a catalyst or in plating processes, additional risks can be associated with the chemicals and processes involved. The alpha-particle irradiation of Rh may produce different, longer-lived silver and rhodium isotopes. The silver radioisotopes from mass number 102 to 106 can be produced on Rh by alpha particle irradiation [1, 2]. The produced radioisotopes have different applications in medicine and industry. ^{103}Ag is a positron emitter and is used in imaging applications. $^{104\,m,g}$Ag, both the ground and the metastable states are of interest in medical applications. One can perform more accurate and efficient tumor treatment by exploiting the diagnostic and therapeutic properties of ^{111}Ag and ^{103}Ag (theranostic pairs) [3, 4]. Ag radioisotopes can also be used to label biomolecules for targeted therapy, enhancing the precision of treatment [4]. The production of a suitable amount of activity from these silver radioisotopes, as well as chemical separation and a proper labeling method, requires further investigations.

From the producible rhodium radioisotopes, ^{99}Rh is used because of its suitable half-life in PET studies and other diagnostic applications. ^{100}Rh is also of interest in PET research. ^{101}Rh is used in Auger-electron therapy (targeted radiotherapy), and ^{102}Rh is also a candidate for PET studies. All these rhodium radioisotopes are used in rhodium chemistry, metallurgy, and as radioactive tracers.

2 Experimental methods

The experiment was performed at the RIKEN AVF cyclotron with a 50 MeV nominal energy alpha beam. The exact beam energy was determined using the time-of-flight (TOF) method [5], and was proven to be 50.8 MeV. The rhodium and titanium foils of different thicknesses (25 and 6 μm

[a] e-mail: ditroi@atomki.hu (corresponding author)

Published online: 08 September 2025

Table 1 Main parameters of the measured radioisotopes

Nuclide	Half-life	Decay mode (%)	E_γ (keV)	I_γ (%)	Contributing reaction	E_{th} (MeV)
^{51}Cr	27.701 d	ε (100)	320.0824	9.91	^{nat}Ti(α,x)^{51}Cr	2.893
^{103}Ag	65.8 min	ε + β^+ (100)	118.74	31.2	^{103}Rh(α,4n)	34.125
			148.2	28.3		
^{104g}Ag	69.2 min	ε + β^+ (100)	555.8	92.6	^{103}Rh(α,3n)	25.478
			767.6	65.7		
^{105g}Ag	41.29 d	ε + β^+ (100)	280.54	31	^{103}Rh(α,2n)	15.138
			644.63	10.2		
^{106m}Ag	8.28 d	ε + β^+	450.976	28.2	^{103}Rh(α,n)	6.947
			717.34	28.9		
^{100g}Rh	20.5 h	ε + β^+ (100)	539.512	80.6	^{103}Rh(α,3nα)	27.489
			822.654	21.09		
^{101m}Rh	4.31 d	ε (92.8) IT(7.2)	306.857	81	^{103}Rh(α,2nα)	17.287
^{102m}Rh	3.742 y	ε + β^+ (99.767)	631.29	56	^{103}Rh(α,nα)	9.752
		β^- (0.233)	697.49	44		
^{102g}Rh	207.3 d	ε + β^+ (78)	468.58	2.9	^{103}Rh(α,nα)	9.611
		β^- (22)	475.06	46		

for Rh and 6 μm for Ti) were purchased from Goodfellow Co., Ltd., UK, and Nilaco Corp., Japan. Irradiation was performed at a beam current of 200 nA for 30 min. We used the well-established stacked foil technique coupled with off-line high-resolution gamma spectrometry for excitation function measurements. The stack was constructed in the sequence of pairs or triplets of foils (Rh–Rh–Ti–Ti or Rh–Rh–Rh–Ti–Ti). For gamma measurement, only the second and downstream foils were used from every pair to avoid the systematic error originating from the recoil effect. The Ti foils served as monitor foils using the ^{nat}Ti(α,x)^{51}Cr monitor reaction. The stack consisted of 24 rhodium and 21 titanium foils, from which only 12 Ti and 13 Rh foils were measured to avoid recoil contribution. The measurements run for about 2 weeks, starting shortly after the end of irradiation, with 10-min-long measurements to catch the short-lived products, and up to 24-h-long measurements to see the long-lived products in several series. Altogether, four series of measurements have been performed for the rhodium foils and one series for the titanium monitor foils.

3 Results and discussion

Four rhodium radioisotopes and four silver radioisotopes were identified in the measured spectra, namely ^{100,101m,102g,102m}Rh, and ^{103,104g,105g,106m}Ag. Based on their half-lives and cross sections, the final data were collected from different measurement series. The nuclear data for these isotopes have been sourced from the NUDAT online database [6, 7] and the Q-value calculator [8], as presented in Table 1. In Table 1, the reaction with the lowest threshold is shown. The cross-section values for the excitation function have been calculated from the measured peak areas and the nuclear parameters. Each peak from each measurement series was evaluated individually, then averaged over the evaluated individual values. The uncertainties were calculated using the error propagation law.

The activation cross sections have been calculated using Eq. (1):

$$\sigma = \frac{\lambda N_\gamma}{\varepsilon_d I_\gamma \varepsilon_t F_t N_b (1 - e^{-\lambda t_i}) e^{-\lambda t_c} (1 - e^{-\lambda t_m})}, \quad (1)$$

where N_γ is the measured net-peak area (counts), λ is the decay constant (s^{-1}), ε_d is the detector efficiency, I_γ is the gamma-ray intensity, ε_t is the dead-time correction parameter, F_t is the surface density of target atoms (cm^{-2}), N_b is the number of projectiles per unit time (s^{-1}), t_i is the irradiation time (s), t_c is the cooling time measured from EOB (End of Bombardment) to the start of the measurement (s), and t_m is the acquisition time (s) (real-time).

The uncertainties of the measured cross sections were calculated by combining the linearly contributing uncertainty components only. The following linear uncertainties were involved: number of target nuclei (3%), number of incident particles (5%), peak area determination including statistical and fitting uncertainty (1–7%), in the case of complex peaks (< 15%), uncertainty of detector efficiency (3–6%), uncertainty of the γ-ray intensity (0.5–10%). The uncertainty of time parameters (half-life, irradiation, waiting and measuring time) was not taken into account. The total uncertainty of

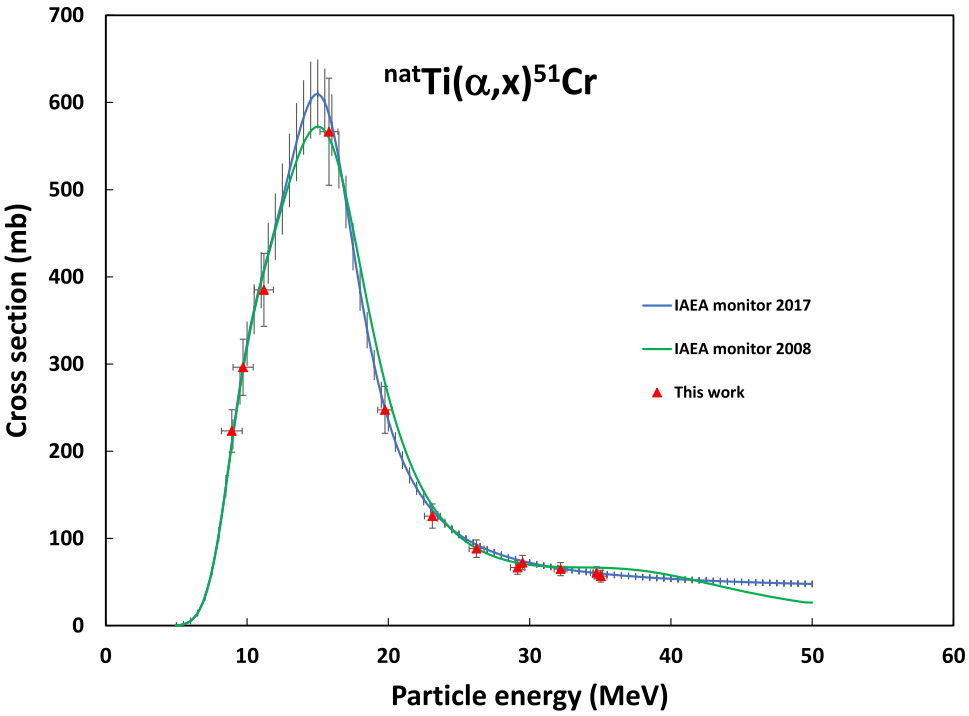


Fig. 1 Measured cross sections of the monitor reaction compared with the two versions of the reference cross section from the IAEA Monitor Reaction database [9]

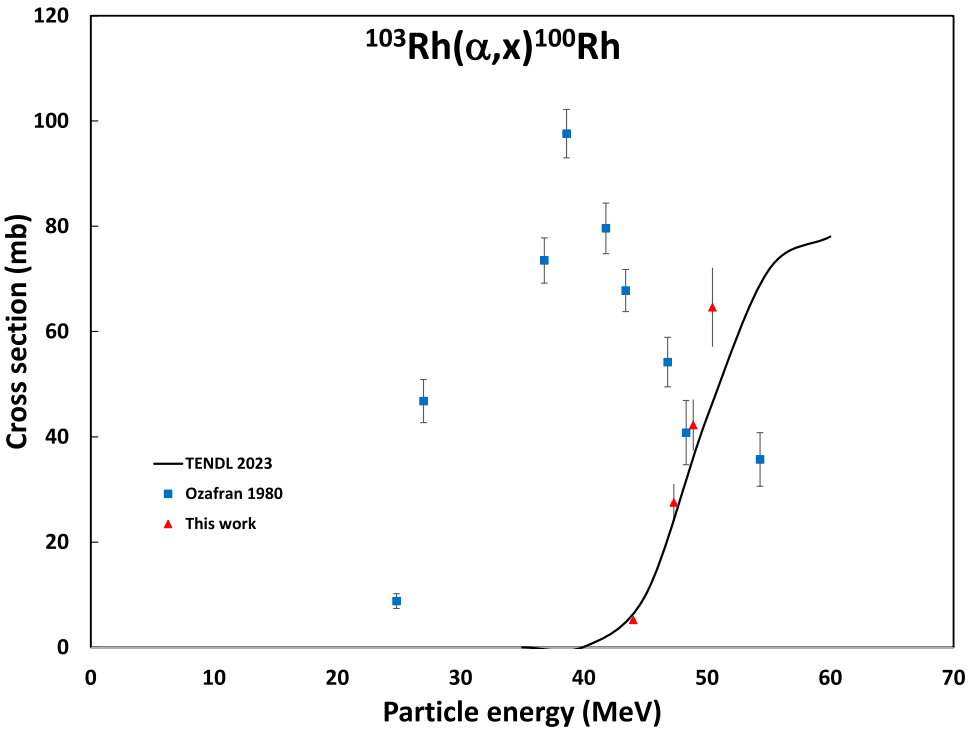


Fig. 2 Measured cumulative excitation function of the ^{103}Rh(α,x)^{100}Rh nuclear reaction compared with the TENDL 2023 prediction and the literature data

the deduced cross sections in this work was between 8 and 12%.

The measured cross sections, together with the TENDL-2023 predictions and the experimental literature data, are presented in Figs. 1, 2, 3, 4, 5, 6, 7, 8 and numerically in Tables 2 and 3.

3.1 ^{nat}Ti(α,x)^{51}Cr monitor reaction

The reference cross-section for this reaction was taken from the IAEA monitor reaction database [9]. The foil thicknesses have been determined (5.21 ± 0.1 μm) and used in the data evaluation instead of the nominal values. The beam intensity was corrected by applying a 0.94 multiplier due to the escape of secondary electrons from the target. In such a way, our

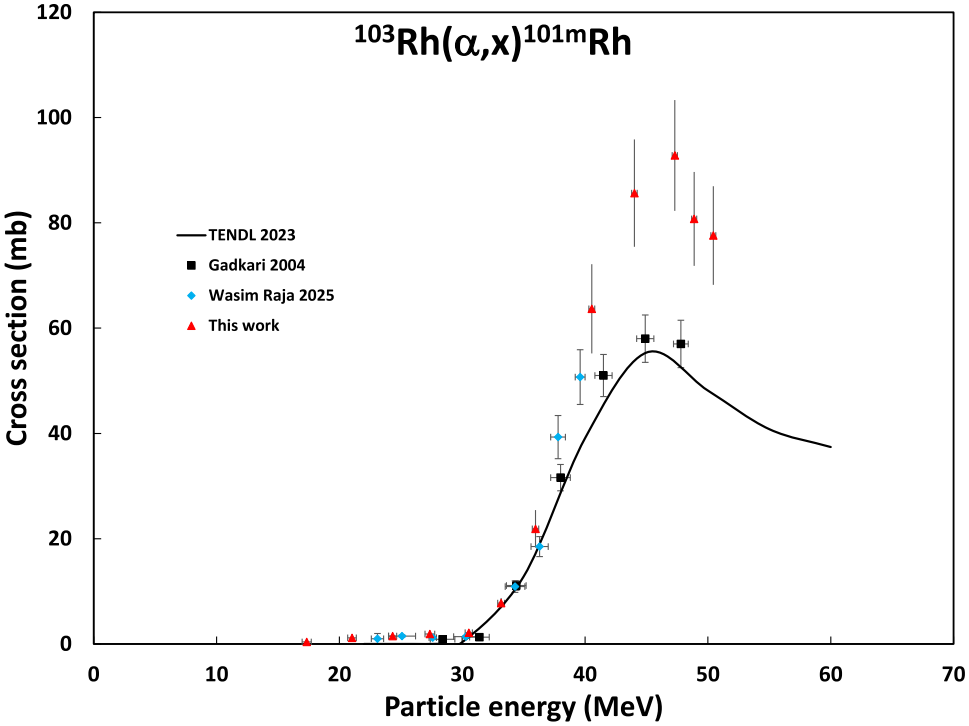


Fig. 3 Measured excitation function of the ^{103}Rh(α,x)^{101m}Rh nuclear reaction compared with the TENDL 2023 prediction and the literature data

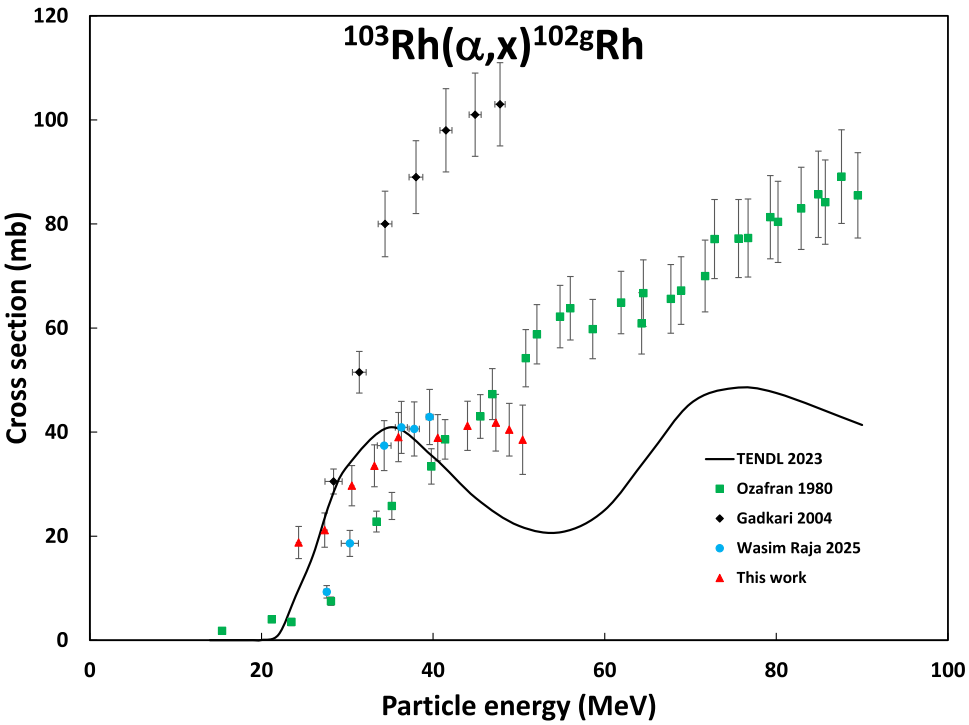


Fig. 4 Measured excitation function of the ^{103}Rh(α,x)^{102g}Rh nuclear reaction compared with the TENDL 2023 prediction and the literature data

measured monitor function shows excellent agreement with both reference curves. We have no measured points at the maximum of the excitation function, where the two reference versions (recommended values) differ from each other.

3.2 ^{103}Rh(α,x)^{100}Rh reaction

We could only measure the $T_{1/2} = 20.5$ h ground-state of the ^{100}Rh (Table 1). The result includes formation by decay of ^{100m2}Rh ($T_{1/2} = 4.6$ min), therefore, the presented data are cumulative. The measured data was evaluated based on the

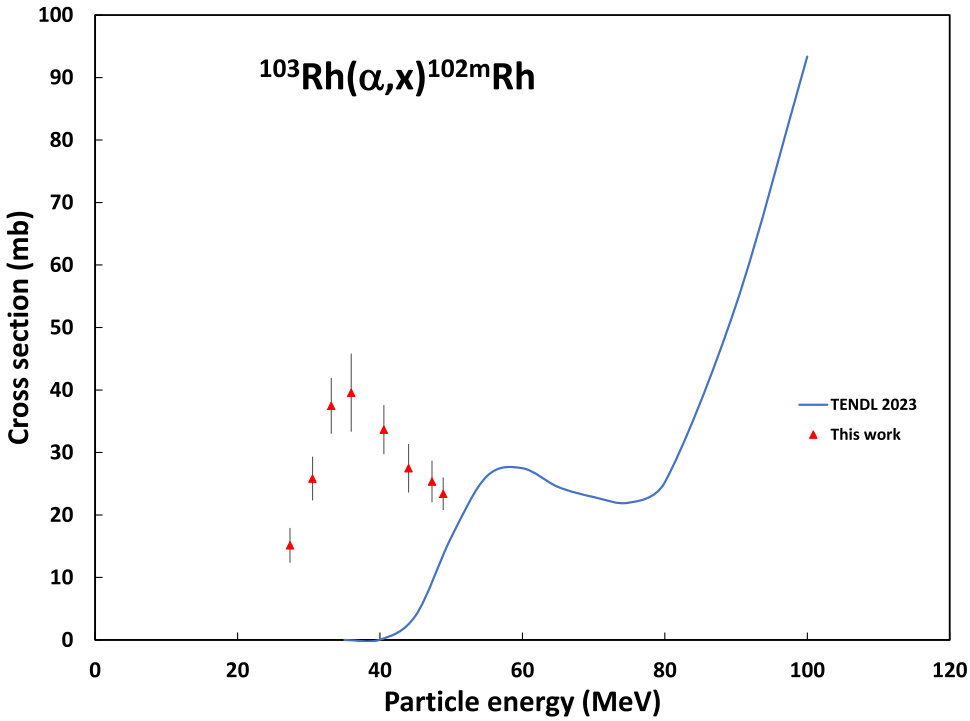


Fig. 5 Measured excitation function of the ^{103}Rh(α,x)^{102m}Rh nuclear reaction compared with the TENDL 2023 prediction

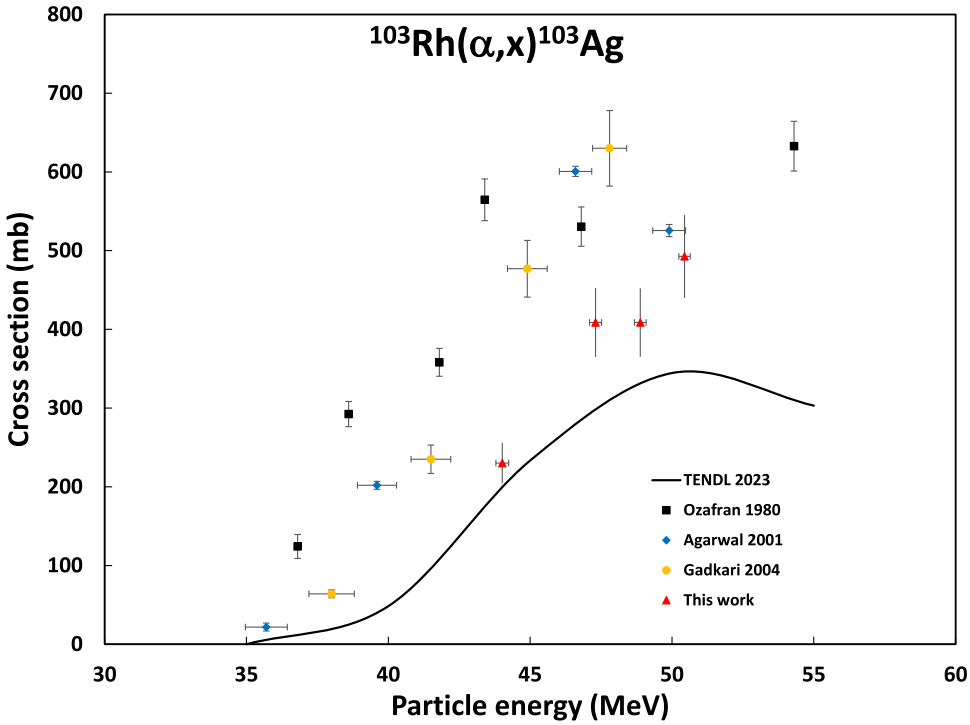


Fig. 6 Measured cumulative excitation function of the ^{103}Rh(α,x)^{103g}Ag nuclear reaction compared with the TENDL 2023 prediction and the earlier literature data

539.512 and 822.654 keV γ-lines, which were detected in all 4 measurement series spectra. The numerical results are presented in Table 3, while the measured excitation function is shown in Fig. 2. One earlier dataset was found in the literature from Ozafran et al. (1980) [10]. Our new data show good agreement with the TENDL 2023 prediction, but the earlier data of Ozafran et al. (1980) has a maximum much higher than ours and TENDL 2023, and the whole function seems to be downwards energy shifted.

3.3 ^{103}Rh(α,x)^{101m}Rh reaction

We could only measure the $T_{1/2} = 4.34$ d isomer of the ^{101}Rh (Table 1). The measured data was evaluated based on the 306.857 keV γ-line, which was detected in all 4 measurement

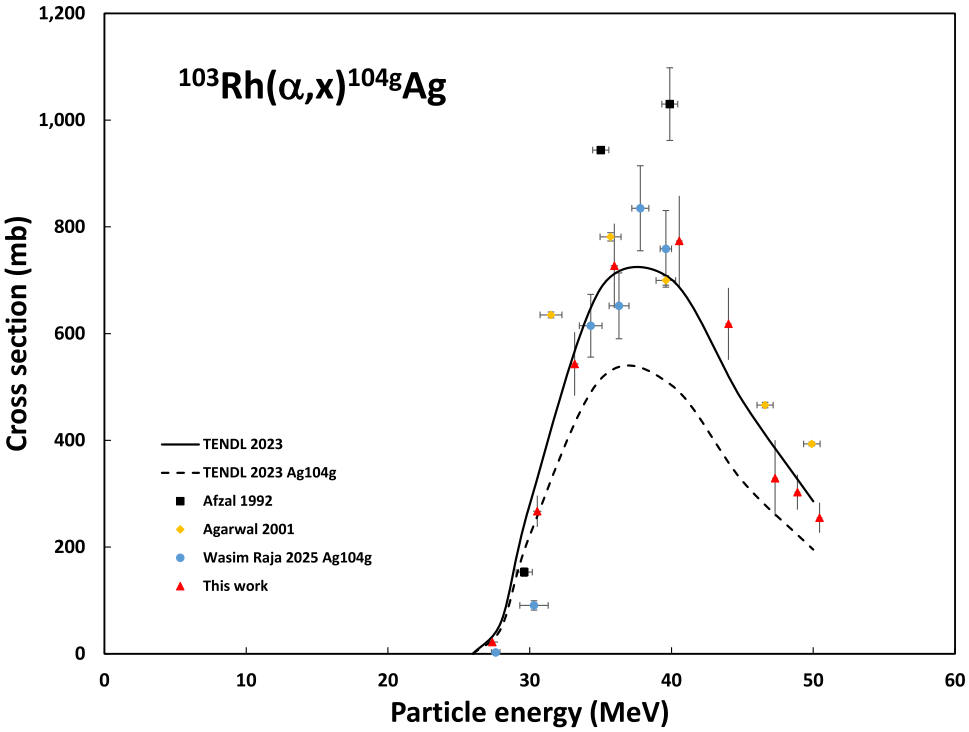


Fig. 7 Measured excitation function of the ^{103}Rh(α,x)^{104g}Ag nuclear reaction compared with the TENDL 2023 prediction and the earlier literature data

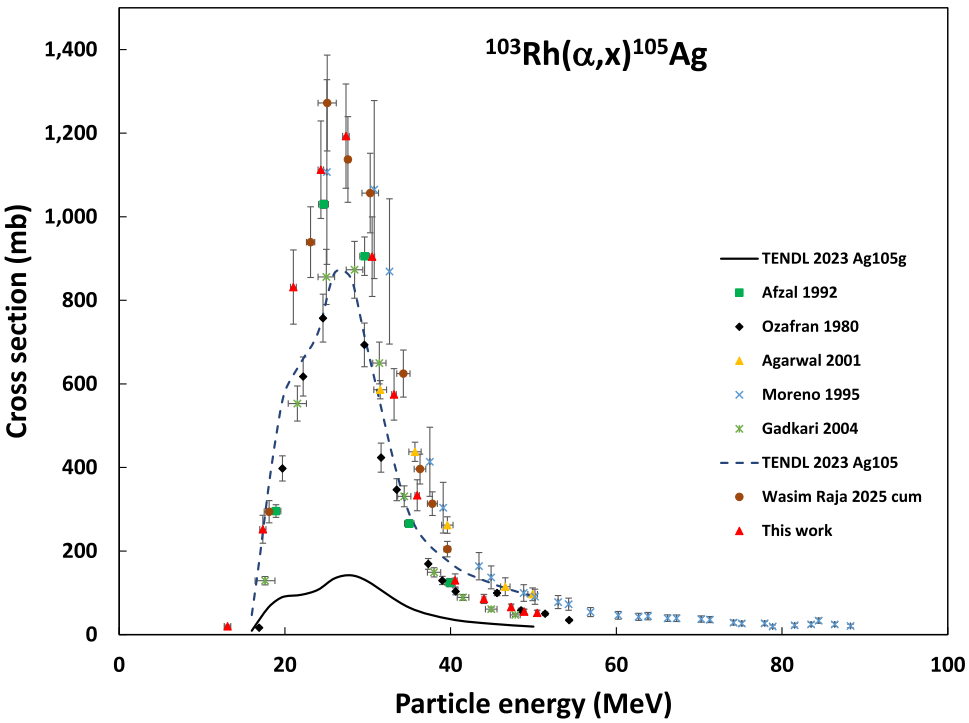


Fig. 8 Measured cumulative excitation function of the ^{103}Rh(α,x)^{105}Ag nuclear reaction compared with the TENDL 2023 prediction and the earlier literature data

series spectra. The numerical results are presented in Table 3, while the measured excitation function is shown in Fig. 3. Two earlier measurements were found in the literature, from Wasim Raja et al. [11] and Gadkari et al. [12]. In Fig. 3, the TENDL 2023 [13] prediction is also shown. Our new data are in good agreement with those of Gadkari et al. (2004) up to 35 MeV and with those of Wasim-Raja et al. up to 40 MeV. TENDL 2023 gives a good trend, but around the maximum, it is much lower than our results.

3.4 ^{103}Rh(α,x)^{102}Rh reaction

From ^{102}Rh we could detect both the ground state ^{102g}Rh ($T_{1/2}$ = 207.3 d) and the ^{102m}Rh ($T_{1/2}$ = 3.742 y) isomeric state. The evaluation of the measured data was made based

Table 2 Measured excitation functions of the silver radioisotopes

Energy (MeV)		Cross section (mb)							
E	dE	σ ^{103}Rh(α,n)^{106m}Ag	dσ	σ ^{103}Rh(α,2n)^{105g}Ag	dσ	σ ^{103}Rh(α,3n)^{104g}Ag	dσ	σ ^{103}Rh(α,4n)^{103}Ag (cum)	dσ
50.44	0.20	2.50	0.4	52.16	6.1	254.9	28.2	492.7	53
48.88	0.21	2.54	0.3	54.98	5.8	302.9	32.8	408.7	43.5
47.31	0.21	3.07	0.4	65.98	7.1	328.9	71.6	408.8	43.9
44.02	0.23	3.68	0.4	85.32	11	618.3	67.4	230.2	25.7
40.55	0.24	4.66	0.5	129.7	15.6	773.6	84.6	56.9	8.3
35.97	0.26	6.69	0.7	333.5	37.1	727	79.2		
33.17	0.28	8.43	0.9	574.9	61.6	543.2	59.4		
30.53	0.29	11.10	1.5	904.4	95	267	29.4		
27.37	0.39	17.32	2	1193	125	22	2.5		
24.33	0.33	35.80	3.9	1113	117				
21.03	0.35	104.1	11	831.7	89				
17.34	0.37	202.7	22	252.2	33.5				
13.07	0.39	28.42	3.1	19.9	3				

Table 3 Measured excitation functions of the rhodium radioisotopes

Energy (MeV)		Cross section (mb)							
E	dE	σ ^{103}Rh(α,x)^{102g}Rh	dσ	σ ^{103}Rh(α,x)^{102m}Rh	dσ	σ ^{103}Rh(α,x)^{101m}Rh	Dσ	σ ^{103}Rh(α,x)^{100}Rh	dσ
50.44	0.20	38.5	6.7			77.6	9.4	64.6	7.5
48.88	0.21	40.5	5	23.4	2.6	80.8	8.9	42.2	4.9
47.31	0.21	41.8	5.5	25.4	3.3	92.8	10.5	27.5	3.5
44.02	0.23	41.2	4.7	27.5	3.9	85.7	10.2	5.2	0.7
40.55	0.24	38.9	4.4	33.7	3.9	63.7	8.5		
35.97	0.26	39	4.7	39.6	6.3	21.9	3.6		
33.17	0.28	33.5	4	37.5	4.5	7.8	1		
30.53	0.29	29.7	3.9	25.8	3.5	2.1	0.4		
27.37	0.39	21.2	3.3	15.1	2.8	1.9	0.3		
24.33	0.33	18.8	3.1			1.5	0.24		
21.03	0.35	45.4	6			1.2	0.16		
17.34	0.37	90.2	10.6			0.4	0.07		
13.07	0.39	11.7	2.2						

on the 475.06 and 468.58 γ-lines for the ground-state and the 631.29 and the 697.49 γ-lines for the isomeric state. Because of the longer half-lives, reliable results could only be extracted from the last series of measurements (longer cooling and longer measuring times). The data of Ozafran et al. [10] are consistent with our data at 40–50 MeV and are smaller at lower energies (Fig. 4). The data of Wasim Raja et al. [11] are consistent with ours at 35–40 MeV and are lower at lower energies. The data of Gadkari et al. [12] are much higher than any of the others above 30 MeV. TENDL 2023 reproduces our ground-state data (Fig. 4) well up to 40 MeV and underestimates all experimental results at higher energies. Our new data for the isomeric state (Fig. 5) are very different from the TENDL 2023 prediction. No other experimental results are available in the literature.

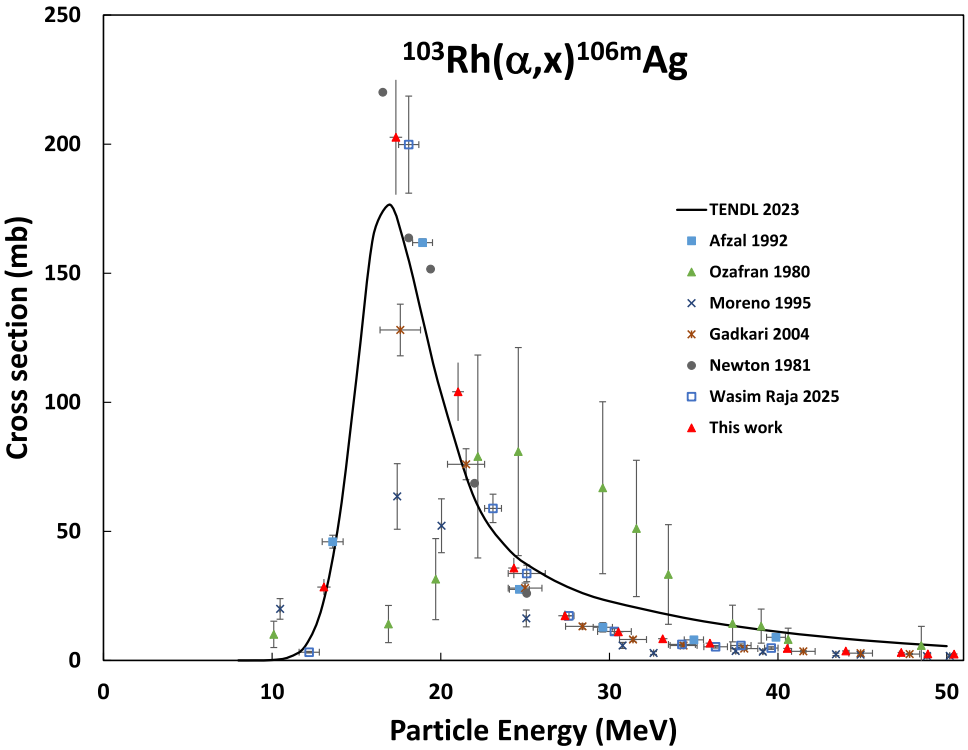


Fig. 9 Measured excitation function of the ^{103}Rh(α,x)^{106m}Ag nuclear reaction compared with the TENDL 2023 prediction and the earlier literature data

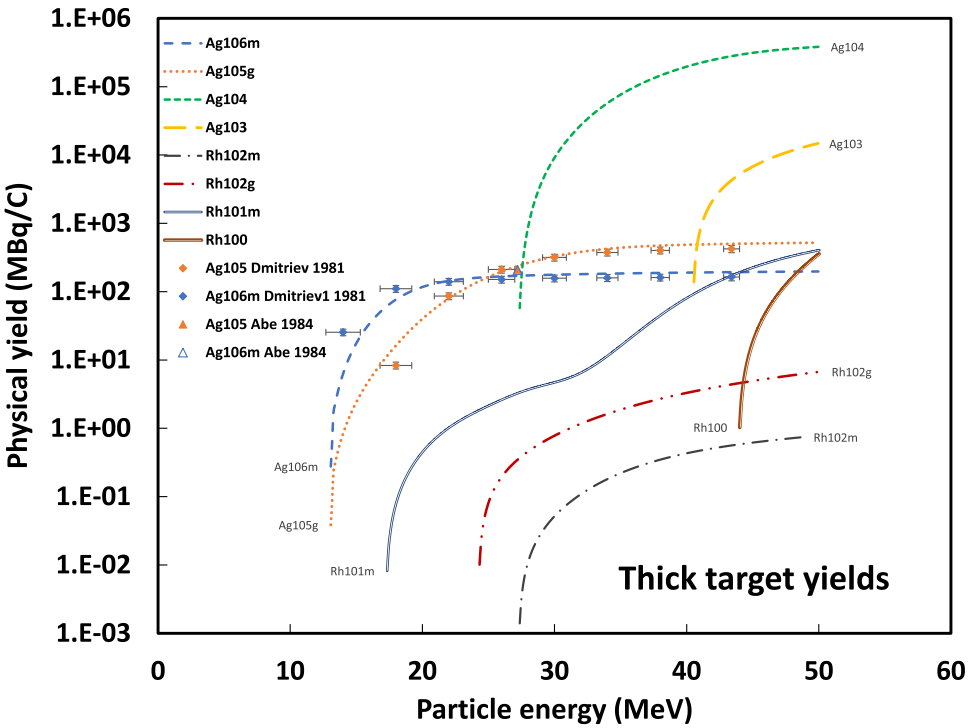


Fig. 10 Physical integral yield calculated from our measured cross-sections, compared with the literature values

3.5 ^{103}Rh(α,x)^{103}Ag reaction

The $T_{1/2} = 5.7$ s excited state of ^{103}Ag could not be caught during the measurement. Only the γ-radiation of the $T_{1/2} = 65.7$ min ground-state was measured. The presented data include formation by decay of the ^{103m}Ag state; therefore, the presented data are cumulative. The evaluation of the measured data was made based on the 118.74 and the 148.2 keV γ-lines. The data (Fig. 6) were taken from the first two series of measurements. Our data are in relatively good agreement with the TENDL 2023 prediction, while the earlier data of Ozafran et al. [10], Agarwal et al. [14], and Gadkari et al. [12] are higher and very scattered.

3.6 ^{103}Rh(α,x)^{104g}Ag reaction

The $T_{1/2} = 33.5$ min excited state of ^{104}Ag could not be analyzed, because of its very low intensity γ-lines. During the measurement, only the γ-radiation of the $T_{1/2} = 69.2$ min ground-state was measured. The evaluation of the measured data was made based on the 767.6 keV γ-line, because the strongest gamma line 556 keV is common with the ^{104m}Ag. The data (Fig. 7) were taken from the first two series of measurements. Our data are in relatively good agreement with the TENDL 2023 prediction, and with the earlier data of Wasim Raja et al. [11] and Agarwal et al. [14]. The data of Afzal et al. [15] are higher than others, especially around the maximum.

3.7 ^{103}Rh(α,x)^{105}Ag reaction

^{105}Ag has the $T_{1/2} = 7.23$ min isomeric state, which decays into the $T_{1/2} = 41.29$ d ground-state, so what we measured is the cumulative cross-section for ^{105}Ag production. The evaluation of the measured data was made based on the 280.54 and the 644.63 keV γ-lines. The data (Fig. 8) were taken from the 2–3 series of measurements. Our data are larger than the TENDL 2023 prediction, and are consistent with the earlier data of Wasim Raja et al. [11], Afzal et al. [15], and Moreno et al. [16]. The data of Ozafran et al. [10] and Gadkari et al. [12] are lower.

3.8 ^{103}Rh(α,x)^{106m}Ag reaction

^{106}Ag has the $T_{1/2} = 23.96$ min ground-state with very weak γ-lines, and the $T_{1/2} = 8.28$ d isomeric state. Only the isomeric state could be detected in our measurements. The measured data was evaluated based on the 450.976 and the 717.34 keV γ-lines. The data (Fig. 9) were taken from the 2–3 series of measurements. Our new data follow the trend of the TENDL2023 prediction and are in relatively good agreement with the earlier results of Afzal et al. [15] and Wasim Raja et al. [11]. The data of Ozafran et al. [10] are completely different from the others and the TENDL 2023, both in trend and amplitude. The data of Gadkari et al. [12] and Newton et al. [17] show only partial agreement with our data. The data set of Moreno et al. [16] extends to 90 MeV and is slightly higher than ours in the overlapping energy region.

3.9 Physical yield calculation

From the measured cross sections, integral physical yields have been calculated for all nuclear reactions (see Fig. 10). The integral thick target yields were calculated by using the formula in Eq. (2) [18, 19].

$$Y_{TT}(E_b) = \frac{\lambda}{Ze} \int_{E_{th}}^{E_b} \frac{\sigma(E)}{S(E)} \tag{2}$$

where λ is the decay constant, Z is the charge state of the bombarding particle (2 for ^{4}He) e is the electron charge, $\sigma(E)$ is the energy dependent cross section, $S(E)$ is the stopping power versus energy E_b is the bombarding energy, E_{th} is the threshold of the nuclear reaction in question. Only Dmitriev et al. [20] and Abe et al. [21] published experimental yield data on ^{105}Ag and ^{106m}Ag. Dmitriev et al. [20] published curves and Abe only single points for both radioisotopes. Their data are in good agreement with our calculated curves (Fig. 10).

4 Conclusion

Within the 50 MeV energy range, a series of medically and technically important silver and rhodium radioisotopes can be produced by alpha-particle induced nuclear reactions with reasonable cross-section/production yield. We have measured and improved the data for the production cross sections of eight radioisotopes, among them the data for ^{102m}Rh is newly obtained. The silver isotopes especially show relatively high yields. Our new measurements confirm and/or reject some earlier experimental results and even give new data in several cases. The comparison with the newest TENDL 2023 predictions helps the TALYS model developers to refine their algorithms.

Acknowledgements This work was carried out at RI Beam Factory operated by RIKEN Nishina Center and CNS, University of Tokyo, Japan. The authors would like to A. Nambu, Y. Shigekawa, Y. Kanayama, H. Shimizu, and S. Mitra (RIKEN Nishina Center) for technical assistance with the experiment. This research was partially performed by the commissioned research fund provided by F-REI (JPFR24040201). The work of the authors F. Ditrói, S. Takács, and Z. Szűcs was partly supported by Project no. NKTA-42, which has been implemented with the support provided by the Ministry of Innovation and Technology of Hungary from the National Research, Development and Innovation Fund, financed under the TKP2021 funding scheme.

Funding Open access funding provided by HUN-REN Institute for Nuclear Research.

Data Availability Statement The new data will be evaluated and uploaded into the EXFOR database.

Code Availability Statement This manuscript has no associated code/software. [Author's comment: Code/Software sharing is not applicable to this article as no code/software was generated or analysed during the current study.]

Declarations

Conflict of interest There is no conflict of interest.

Ethics statement It is testified on behalf of all co-authors that our article submitted followed ethical principles in publishing.

Open Access This article is licensed under a Creative Commons Attribution 4.0 International License, which permits use, sharing, adaptation, distribution and reproduction in any medium or format, as long as you give appropriate credit to the original author(s) and the source, provide a link to the Creative Commons licence, and indicate if changes were made. The images or other third party material in this article are included in the article's Creative Commons licence, unless indicated otherwise in a credit line to the material. If material is not included in the article's Creative Commons licence and your intended use is not permitted by statutory regulation or exceeds the permitted use, you will need to obtain permission directly from the copyright holder. To view a copy of this licence, visit http://creativecommons.org/licenses/by/4.0/.

References

1. M. Choudhary, N. Singh, M. Upadhyay, P. Dubey, S. Singh, S. Paul, U. Mishra, S. Dasgupta, J. Datta, A. Kumar, Excitation functions for natAg(α,x) reactions with detailed covariance analysis. Nucl. Phys. A **1050**, 122917 (2024)
2. L. Kidd, Curies for patients. Nucl. Eng. Int. **53**(648), 26–32 (2008)
3. M. Tosato, M. Asti, Lights and shadows on the sourcing of silver radioisotopes for targeted imaging and therapy of cancer: production routes and separation methods. Pharmaceuticals **16**(7), 929 (2023)
4. M. Tosato, A. Gandini, S. Happel, M. Bas, A. Donzella, A. Zenoni, A. Salvini, A. Andrighetto, V.D. Marco, M. Asti, Chromatographic separation of silver-111 from neutron-irradiated palladium target: toward direct labeling of radiotracers. EJNMMI Radiopharm. Chem. **8**, 43 (2023)
5. T. Watanabe, M. Fujimaki, N. Fukunishi, H. Imao, O. Kamigaito, M. Kase, M. Komiyama, N. Sakamoto, K. Suda, M. Wakasugi, K. Yamada, Beam energy and longitudinal beam profile measurement system at RIBF, in *5th International Particle Accelerator Conference (IPAC2014)*, Dresden, Germany (2014). https://doi.org/10.18429/JACoW-IPAC2014-THPME136
6. BNL, NUDAT, Decay data retrieval code (Brookhaven National Laboratory, USA, 2023) [Online]. http://www.nndc.bnl.gov/nudat3/ [Accessed 2024].
7. M. R. Bhat, NUDAT 2.6. Nuclear Data Sheets **88**(3), 417 (1999).
8. B. Pritychenko, A. Sonzogni, Q-value calculator. BNL (2003) [Online]. http://www.nndc.bnl.gov/qcalc [Accessed 2025].
9. IAEA, IAEA cross section database for beam monitor reactions (2024) [Online]. https://nds.iaea.org/medical/monitor_reactions.html [Accessed 2024].
10. M. Ozafran, M. Vazquez, M. De La Vega Vedoy, S. Nassiff, Excitation functions and thick target yields of (a,xn) and (a,axn) reactions on Rh-103. Radiochem. Radioanal. Lett. **43**, 265 (1980).
11. S. Wasim-Raja, R. Acharya, A. Saha, Experimental measurements and theoretical calculations of excitation functions of ^{103}Rh(α,xn)^{106m,105g,104g}Ag and ^{103}Rh(α,αxn)^{101m,102g}Rh reactions up to 40 MeV. Nucl. Phys. A **1053**, 122974 (2025)
12. M. Gadkari, N. Singh, Alpha-particle induced reactions on rhodium. Pramana J. Phys. **62**, 1059 (2004)
13. TENDL2023 (2023) [Online]. https://tendl.web.psi.ch/tendl_2023/tendl2023.html [Accessed 2024].
14. A. Agarwal, M. Bhardwaj, I. Rizvi, A. Chaubey, Equilibrium and pre-equilibrium studies in some alpha induced reactions on rhodium. J. Phys. Soc. Japan **70**, 2903 (2001)
15. M. Afzal Ansari, N. Sathik, B. Singh, M. Sankaracharyulu, R. Prasad, Study of excitation functions in Rh(alpha,xn)Ag reactions. Int. J. Mod. Phys. Part E **5**, 345 (1996).
16. A. Moreno, J. Massotta, A. Barral, S. Nassiff, Silver isotopes produced by alpha-particles on rhodium. J. Radioanal. Nucl. Chem. **198**, 41 (1995)
17. G. Newton, V. Robinson, E. Shaw, Rh-103(a,xn)Ag-107-X reactions. J. Inorg. Nucl. Chem. **43**, 2227 (1981)
18. M. Aikawa, S. Goto, D. Gantumur, D. Ichinkhorloo, U. Ukon, N. Otuka, S. Takács, H. Haba, Activation cross sections of 7Li-induced reactions on natTi: implications for monitor reactions. Nucl. Instrum. Methods Phys. Res. Sect. B Beam Interact. Mater. Atoms **559**, 165579 (2025)
19. N. Otuka, S. Takács, Definitions of radioisotope thick target yields. Radiochim. Acta **103**(1), 1 (2015)
20. P.P.P. Dmitriev, M. Panarin, Z. Dmitrieva, Yields of Ag-105, Ag-106-m, Ag-108-m, Ag-110-m and Ag-111 in reactions with protons, deuterons and alpha-particles. Sov. Atomic Energy **50**, 388 (1981)
21. K. Abe, A. Iizuka, A. Hasegawa, S. Morozumi, Induced radioactivity of component materials by 16-MeV protons and 30-MeV alpha particles. J. Nucl. Mater. **123**, 972 (1984)